

# Identification of the Limiting Mechanism in Contact Drying of Agitated Sewage Sludge

Patricia Arlabosse, T. Chitu

► **To cite this version:**

Patricia Arlabosse, T. Chitu. Identification of the Limiting Mechanism in Contact Drying of Agitated Sewage Sludge. *Drying Technology*, Taylor & Francis, 2007, 25 (4), pp.557-567. <10.1080/07373930701226955>. <hal-01165249>

**HAL Id: hal-01165249**

**<https://hal-mines-albi.archives-ouvertes.fr/hal-01165249>**

Submitted on 18 Jun 2015

**HAL** is a multi-disciplinary open access archive for the deposit and dissemination of scientific research documents, whether they are published or not. The documents may come from teaching and research institutions in France or abroad, or from public or private research centers.

L'archive ouverte pluridisciplinaire **HAL**, est destinée au dépôt et à la diffusion de documents scientifiques de niveau recherche, publiés ou non, émanant des établissements d'enseignement et de recherche français ou étrangers, des laboratoires publics ou privés.

# **IDENTIFICATION OF THE LIMITING MECHANISM IN CONTACT DRYING OF AGITATED SEWAGE SLUDGE**

**P. Arlabosse and T. Chitu**

Ecole des Mines d'Albi Carmaux, 81013 Albi CT Cedex 9, France<sup>1</sup>

## **ABSTRACT**

In spite of a great number of industrial applications, the thermal design of contact dryers for sewage sludge remains empirical. To improve the understanding of drying mechanisms, the penetration theory developed by Schlünder and co-workers for mono and multi dispersed packing is used to represent the experimental results from a laboratory scale dryer. For granular packing, the only adjustment parameter of the model is the mixing number, which characterizes the dryer and its stirrer. For pasty-like materials, the pasty phase is assumed to be a saturated particulate phase. As the calculation of the effective properties calculation is cumbersome for a multi-granular packing, the particulate phase is considered as a mono-dispersed packing, whose dimension is unknown. To identify the two adjustment parameters, the mixing number was quantified from experiments performed on activated alumina balls, for which physical and thermal characteristics are known, and then the characteristic dimension of

---

<sup>1</sup> Correspondence : P. Arlabosse, Centre RAPSODEE (UMR 2392), Ecole des Mines d'Albi Carmaux, Route de Teillet, 81013 Albi CT Cedex 09, France. Tel : +33563493237. Fax : +33563493243

the sludge was determined by adjustment of experimental drying kinetics measured in a batch agitated dryer. According to this model, drying is exclusively controlled by the contact resistance between the wall and the biggest particles contained in the dewatered sludge. The model allows to find most of the tendencies experimentally observed for different operating conditions.

Key Words: contact drying, mixing, drying kinetic, sludge, activated alumina, on site measurement

## INTRODUCTION

The constituents removed in a wastewater treatment plants (WWTP) include screenings, grit, scum, as well as solids and bio-solids that both are called “the sludge”. Of all these constituents, sludge is the largest by volume, and around 1,000,000 tons of sludge (measured as dry matter) is generated each year in the French municipal WWTP. After mechanical dewatering, these solids and bio-solids have a lumpy appearance and, usually, contain from 16 to 30 percent of solid matter by weight. Thermal drying is positioned as an intermediate unit operation which allows to process the sludge to a product that can easily be handled, stored and reused in agriculture or incineration. Since indirect dryers have lower energy consumption and running cost than direct ones as well as a lesser environmental impact, we focus our attention on this type of dryers. In spite of a great number of industrial applications, their design remains empirical. A bottom up methodology [1] has been developed to improve the thermal design of paddle dryers:

- ✓ At the lab scale, drying experiments are performed in a batch agitated vertical dryer [2]. The drying kinetics and the evaporation flow rates are computed from an energy balance;

- ✓ The data collected are then used to compute the moisture content distribution along the industrial dryer.

Using this methodology, a classification of the sludge according to their capacity to be dried in a paddle dryer was established [3]. Samples coming from different WWTP, where different wastewater treatment processes are implemented, were characterized and dried in the batch dryer. Primary sludges lead to the lowest drying rates while appreciably identical drying rates were obtained for extended aeration and digested sludges. The same classification is achieved when considering the infrared spectra of the dry sludge samples, recorded using a coupled TG-FTIR and treated by Principal Component Analysis to reduce the dimensionality of the data set. This "black box" approach shows that it is possible to establish a typology of the sludge but, considering the composition of the product, the allocation of the absorption bands to a particular compound is difficult. As a consequence, a simulation based on the penetration model was initiated [4] to improve our understanding of the drying mechanisms and the thermal design of contact dryers with agitation for pasty materials.

Developed to describe the heat transfer from heated surfaces to dry moving packings [5], the model rests on the description of the random particle motion effect. The continuous mixing process is replaced by a sequence of unsteady mixing steps. During a fictitious period  $t_R$ , the bulk is assumed to be static. Thereafter, an instantaneous perfect macro-mixing of the bulk occurs, followed by the same static period again. This is the so-called penetration theory. For its application to drying, a drying front is assumed to penetrate from the hot surface into the bulk during the static period. When this period ends, the bulk is perfectly mixed and thereafter the drying front moves again into the bulk. The apparent resting time,  $t_r$ , is a mechanical property of the system and function of the dryer type, of the stirrer (form and speed). This apparent resting time is defined as the ratio of a mixing number,  $N_{mix}$ , which indicates how often the stirrer must have turned around before the product has been ideally mixed, to the number of revolutions per second of the stirrer. This mixing number must be fitted to experimental results or calculated using empirical power laws [6], which correlate the mixing number to the Froude one,  $Fr$ .

This model was first used for contact drying of free flowing monodispersed granular material under vacuum conditions [6] or in the presence of inert gases [7]. The contact resistance between heated walls and particles is rate controlling for coarse particles whereas the penetration resistance of the bulk is rate controlling for fine particles.

The influence of particle size distribution on the drying rate for multi-granular packing was discussed by Tsotsas and Schlünder [8]. When de-mixing occurs, the experimental drying rate exhibits a bend point, whose location is directly proportional to the proportion of fine product in the bed. A model was specifically developed for drying of bi-dispersed packings and experimentally validated. The drying process comprises two successive steps: (i) drying of the fine particles forming a layer in contact with the heating plate (according to the model proposed by Schlünder and Mollekopf [6]) and (ii) drying of the coarse layer lying on the fine one, assuming that the fine particles are dry and at a temperature higher than the saturation temperature of the coarse particles. When de-mixing does not occur, an elementary unit of the structure has to be assumed to calculate the effective properties of the stochastic homogeneous multi-granular packings. The authors emphasized that the calculation becomes rapidly cumbersome. As a consequence, a model was only developed for homogeneous bi-dispersed packings but not validated. According to this theoretical model, the presence of fine particles tends to increase the drying rate.

A few years ago, Dittler et al. [9] extended the penetration theory to pasty materials, like aqueous suspension of china clay, considered as a saturated particulate phase. With the assumption that the dry product in the paste regime is the same as the comminuted fine dry product in the granular regime, the drying rate is calculated for the pasty and particulate regimes in the same way using one of the previously described models. Whatever the application, drying was assumed to be a purely heat transfer controlled process, either by the contact resistance at the heated wall or by the bulk heat transfer resistance.

An approach similar to that of Dittler et al. [9] was developed to compute the drying kinetics of the municipal sewage sludge dried in the laboratory contact dryer and to identify the limiting mechanism.

## ASSUMPTIONS

### Sludge modeling

The extension of the penetration theory to paste-like products considers that the pasty phase is a saturated particulate phase. In other words, the dry product in the paste regime is assumed to be the same as the dry product in the granular regime. Unfortunately, the drying process is both a dewatering process and a solid forming process with a "reverse granulation" phase from the wet to the dry solid. As a consequence, the particle size distribution evolves during drying. Mechanically dewatered sludges, which have pasty consistencies, are multi-dispersed materials with particle size distribution ranging from some micrometers to a millimeter (see Figure 1). During drying, the pasty material undergoes a sticky phase before the granular phase appears in the dryer. At that time, the particle size distribution of the moist product ranges from hundred of micrometers to some millimeters. During the last stage of drying, attrition occurs. Besides the residence time of the particles in the dryer, the attrition phenomenon depends on the sludge origin, the stirrer geometry, its rotational speed and the dryer geometry [3]. To compute the drying kinetics through the penetration theory, a multi-granular packing model with a time dependent particle size distribution would be required. Since the experimental drying rate curves [1] do not exhibit a bend point which can be attributed to a segregation phenomenon, it could be assumed that mixing is not accompanied with de-mixing. This hypothesis seems all the more justified as sewage sludges are highly sticky products [10]. As a result, a stochastic homogeneous multi-granular packing model [8] would be sufficient. Nevertheless, calculations of the packing effective properties, such as the effective thermal conductivity, are cumbersome, even for bi-dispersed packings. To avoid cumbersome calculations resulting from a stochastic homogeneous multi-granular packing with time-dependent particle size distributions, it was decided to represent sewage sludges by a saturated mono-dispersed particulate phase

and to determine the characteristic dimensions, used to compute the drying rate both in the pasty and granular regimes, by adjusting the experimental drying rate curves.

#### Convective heat flux

A part of the heat flux supplied to the sludge in the lab dryer results from the flow of superheated vapor, used as a sweeping gas, above the free surface of the product. Experiments [11] performed with different superheated vapor temperatures showed (see Figure 2) that the contribution of forced convection is weak during the periods where the heated surface of the dryer is fully covered by the sludge, i.e., during the pasty and granular regimes. Only the intermediate regime undergoes the influence of the forced convection. This regime is a consequence of the vertical design of the lab scale dryer. As drying progresses, the sludge becomes sticky. Due to the dryer geometry, the sludge accumulates in dead volumes or sticks to the stirrer and the contact between the sludge and the dryer wall is imperfect. As a result, the sludge is mainly dried by convection from superheated vapor and conduction through the stirrer. It was demonstrated that this regime observed at the lab scale is not representative of the drying mechanisms in an industrial paddle dryer [1]. As a consequence, we will not try to model the drying mechanisms involved in this intermediate regime and, in the following, the convective heat transfer at the free surface of the product will be neglected in view of the conductive heat transfer through the heating wall.

#### Permeation resistances and penetration resistance of the particles

The permeation resistance of the bulk is generally weak for static beds and almost zero when packings are mechanically mixed [6]. This resistance will be neglected in the following. Like in publications by Schlünder and coworkers, the penetration and permeation resistances of the particle will be neglected in a first attempt. Vapor is used as sweeping gas during contact drying experiments so that no mass transfer resistance should be taken into account in the gas phase.

## Sludge hygroscopicity

Within the framework of this work, the hygroscopic behavior of the material ([12]; [13]) will be taken into account through the evolution of the total heat of desorption,  $\Delta H_{\text{total}}$ , with the average moisture content of the bed,  $X$ .

## DRYING MODEL FOR CONTACT DRYING OF AGITATED SEWAGE SLUDGE

Considering the hypotheses previously formulated, the model postulates that contact drying is a purely heat transfer controlled process with two remaining “in series” resistances during the stagnation period, when the drying front penetrates into the bulk. These two resistances are the contact resistance and the penetration resistance of the bulk, which can be calculated [6] from the kinetic theory of gases and from Fourier’s theory, respectively. Here are the main stages of the calculation procedure.

The expression of the contact resistance,  $R_{\text{contact}}$ , is provided by equation (1):

$$R_{\text{contact}} = \left[ \Phi \alpha_{\text{w-p}} + (1 - \Phi) \frac{2 k_v / d}{\sqrt{2} + (2l + 2\delta) / d} + 4 C_{12} T_m^3 \right]^{-1} \quad (1)$$

where  $\Phi$ ,  $d$ ,  $\delta$ ,  $T_m$ ,  $k_v$  are the surface coverage factor, the particle size, the surface roughness of the particle, the mean temperature between the wall and the first layer of particles, the thermal conductivity of the vapor, respectively.  $\alpha_{\text{w-p}}$  is the heat transfer coefficient between the heated wall and one particle of the static packing, defined as follows:

$$\alpha_{\text{w-p}} = \frac{4 k_v}{d} \left[ \left( 1 + \frac{2l + 2\delta}{d} \right) \ln \left( 1 + \frac{d}{2l + 2\delta} \right) - 1 \right] \quad (2)$$

$l$  is the modified mean free path of the gas molecules given by equation (3):



$$l = 2 \frac{2-\gamma}{\gamma} \left( \sqrt{\frac{2\pi \tilde{R} T_m}{M}} \frac{k_v}{P(2C_{p,v} - \tilde{R}/M)} \right) \quad (3)$$

where  $\gamma, \tilde{R}, M, P, C_{p,v}$  are the accommodation coefficient, the gas constant, the molecular weight, the pressure and the specific heat of the vapor, respectively.

Finally,  $C_{12}$  is the overall radiation coefficient, defined as follows :

$$C_{12} = \frac{\sigma}{1/\varepsilon_w + 1/\varepsilon_b - 1} \quad (4)$$

where  $\sigma, \varepsilon_w, \varepsilon_b$  are the black body radiation coefficient, the emissivities of the wall surface and the bed surface.

The penetration resistance is obtained by resolution of Fourier's equation for a moving front. Neumann's solution of Fourier's equation for constant wall temperature supplies the temperature profiles between the hot surface and the drying front for each static period as well as the position of the drying front. Both allows to calculate the penetration resistance according to:

$$R_{\text{penetration}} = \frac{R_{\text{contact}} \sqrt{\pi \tau_r} \operatorname{erf}(z_{\text{adim}})}{2} \quad (5)$$

where  $\tau_r$  and  $z_{\text{adim}}$  are the non dimensional apparent resting time and the non dimensional drying front position, respectively defined by equation (6) and (7):

$$\tau_r = R_{\text{contact}}^{-2} \left( k \rho C_p \right)_{\text{db}}^{-1} t_r \quad (6)$$

$$z_{\text{adim}} = \frac{z}{2\sqrt{a_b t}} \quad (7)$$

The apparent resting time,  $t_r$ , which appears in equation (6), must be calculated from an empirical power law, which correlates the mixing number to the Froude number,  $Fr$ , as follows:

$$t_r = \frac{N_{\text{mix}}}{n} = \frac{\psi Fr^\xi}{n} = \frac{\psi}{n} \left( \frac{(2\pi n)^2 D}{2g} \right)^\xi \quad (8)$$

where  $N_{mix}$ ,  $n$ ,  $g$ ,  $D$  are the mixing number, the number of revolution of the stirrer, the gravitational constant and the dryer diameter, respectively.  $\Psi$ ,  $\xi$  are two adjustment constants.

The non dimensional drying front position is the solution of equation (9):

$$\sqrt{\pi} z_{a\ dim} \exp\left(z_{a\ dim}^2\right) \left[1 + \left(\sqrt{\pi}/2\right) \sqrt{\tau_r} \operatorname{erf}\left(z_{a\ dim}\right)\right] = \frac{\left(\sqrt{\pi}/2\right) \sqrt{\tau_r}}{X \Delta H_{total}} C_{p,db} (T_w - T_b) \quad (9)$$

where  $X$ ,  $C_{p,db}$ ,  $T_w$ ,  $T_b$  are respectively the moisture content, the specific heat of the dry bed, the wall temperature and the bulk temperature, respectively.

Finally, the global resistance,  $R_{global}$ , is given by equation (10):

$$R_{global} = R_{contact} + R_{penetration} = \left(1 + \frac{\sqrt{\pi \tau_r} \operatorname{erf}\left(z_{a\ dim}\right)}{2}\right) R_{contact} \quad (10)$$

Knowing this resistance, the heat fluxes exchanged at the heated wall and at the drying front can be calculated. The difference between these two values corresponds to the thermal power absorbed by the dry product. Assuming no heat transfer between dry and wet particles during the instantaneous perfect macro-mixing of the bulk, the drying rate,  $F$ , and the bulk average temperature increase during each static phase,  $\Delta T_{bulk}$ , can be given as:

$$F = \frac{(T_w - T_b) \exp\left(-z_{a\ dim}^2\right)}{R_{global} \Delta H_{total}} \quad (11)$$

$$\Delta T_b = \frac{\Delta H_{total}}{C_{p,db} + X C_{p,wat}} \frac{1 - \exp\left(-z_{a\ dim}^2\right)}{\exp\left(-z_{a\ dim}^2\right)} \Delta X \quad (12)$$

where  $\Delta X$  is the decrement of moisture content during the static phase.

As a result, the model allows to calculate the drying rate curve and the evolution of the average bed temperature knowing:

- ✓ the apparent resting time, which is characteristic of the dryer;

- ✓ the operating conditions (wall temperature, pressure, stirrer speed);
- ✓ the initial moisture content of the product, its total heat of desorption and the dry mass;
- ✓ the particle size and its rugosity;
- ✓ the density, the thermal conductivity and the specific heat of the dry product;
- ✓ the thermal conductivity and the specific heat of the vapor phase;
- ✓ the covering factor and the emissivity of the wall.

## SENSITIVITY ANALYSIS

A sensitivity study of the drying rate  $F$  to variations of the model parameters has been performed. This allows identification of the most influential parameters and the range of moisture content for which the drying rate is sensitive to this parameter. This study was realized for the parameters previously quoted, with the exception of the initial moisture content, the dry mass, the total heat of desorption and the properties of the vapor, supposed to be known exactly. The sensibility coefficient,  $SF_j$ , of the drying rate  $F$  to a parameter  $\beta_j$  is a partial derivative of the function  $F=F(\beta)$  with regard to  $\beta_j$ :

$$SF_j = \frac{\partial F(\beta_j)}{\partial \beta_j} \quad (13)$$

The reduced sensitivity coefficient,  $SF_j'$ , of the drying rate  $F$  to a parameter  $\beta_j$  is computed by finite difference as:

$$SF_j' = \beta_j \frac{F(\beta_j + \delta\beta_j) - F(\beta_j - \delta\beta_j)}{2\delta\beta_j} \quad (14)$$

The use of reduced coefficients, which have the dimension of a drying rate, allows the influence of different parameters to be directly compared. Secondly, a negative (respectively a positive) value of  $SF_j'$

means that an increase of the parameter  $\beta_j$  results in a decrease (respectively an increase) of the drying rate  $F$ .

Reduced sensitivity coefficients to parameters connected with operating conditions and wall characteristics are plotted in Figure 3 whereas those deriving from parameters connected with product properties are plotted in Figure 4. At high moisture content ( $X > 0.7 \text{ kg/kg}$ ), the most influential parameters are the wall temperature, the covering factor and the particle diameter. At low moisture content ( $X < 0.7 \text{ kg/kg}$ ), the wall temperature remains the most influential parameter followed by the stirrer speed and the thermal conductivity or the density of the bulk, these two parameters being correlated. More specifically, an increase of the wall temperature results in an increase of  $F$  whereas an increase of the particle diameter leads to a decrease of  $F$ . As expected with regard to the working temperatures,  $C_{12}$  has little influence on  $F$ . Finally, the specific heat of the dry sludge has practically no influence on  $F$ . Since reduced sensitivity coefficients to  $T_w, \Phi, d, n, k_{bed}$  are high, a good knowledge of these parameters is crucial.

## **DETERMINATION OF THE MODEL PARAMETERS**

Macroscopic parameters bound to the sludge

Experiments were performed with the sewage sludge coming from the municipal wastewater treatment plant (WWTP) from Albi city, which has a capacity of 65 000 population equivalents. In this WWTP, the biological sludge is mixed with the primary sludge before being stabilized in the mesophilic anaerobic digester and mechanically dewatered. Its initial moisture content is 5.2 kg of water/kg of dry matter.

A thermogravimetric analyzer (TGA) coupled with a differential scanning calorimeter DSC111 (Setaram, Caluire, France) used in isothermal mode enables a direct and continuous measurement of the total heat of sorption as a function of the moisture content [14]. Experimental data are then adjusted according to equation (15):

$$\Delta H_{\text{total}} = L_v + 2.110^6 \exp(-A * X) \quad (15)$$

with  $A=10$  for this digested sewage sludge.

Among the properties of the dry packing, only the thermal conductivity has a significant influence on the drying rate. Theoretical models [15] and power law correlations [16] are available in the literature to compute the thermal conductivity from the particle size distribution and factors of shape. But the complex composition of sewage sludge practically precludes the application of these theoretical models. Indeed, the activated sludge is a mixture of water, suspended particles, organic and inorganic colloids, fibers, micro-organisms, biopolymers stemming from the biologic synthesis, ions etc. As a consequence, the order of magnitude of thermal conductivity has to be determined experimentally. The extended hot wire method [17] is used to determine the volumetric thermal capacity,  $\rho C_p$ , and the thermal conductivity,  $k$ , from the measured temperature rise in the sample heated by a Joule effect heat flux. The accuracy on the bulk thermal conductivity is estimated to 5%. Finally, the specific heat of the dry sludge could be measured using a C80 Setaram calorimeter (Setaram, Caluire, France). Data measured at 25°C are reported in **Erreur ! Source du renvoi introuvable.**

As mentioned previously, the characteristic dimension  $d$ , used to compute the drying rate both in the pasty and granular regimes, is unknown and will be determined by adjustment of the experimental drying kinetic. The surface roughness of the particles,  $\delta$ , is unknown, as well. Since the sensibility analysis emphasizes that this parameter has a weak influence on the drying kinetics, its value was fixed according to the literature ([6]; [18]).

#### Parameters bound to the dryer

Experiments were performed in a laboratory batch dryer with a vertical agitator, especially designed and instrumented to monitor the dryer wall temperature, the product temperature, the drying kinetic as well as the mechanical torque. The wall temperature and the stirrer speed are measured with 0.12% and

1% accuracy, respectively. The value suggested by Schlünder and Mollekopf [6] for the wall covering factor,  $\Phi=0.8$ , is used in a first attempt.

The mixing number  $N_{\text{mix}}$  characterizes the dryer and its stirrer.  $N_{\text{mix}}$  could be calculated using empirical power laws [6], which correlate the mixing number to the Froude one (see equation 8) through two adjustment constants,  $\Psi$  and  $\xi$ . For a similar dryer configuration, Schlünder and Mollekopf [6] suggest  $\Psi = 25$  and  $\xi = 0.2$ . Since this number is the only adjustment parameter of the model for mono-dispersed granular packing,  $N_{\text{mix}}$  could also be fitted to experimental results. Experiments were performed with mono-dispersed granular packing of activated alumina balls (Caldic, Bobigny, France), shaped as porous spherical beads, for various particles diameters ( $1 \leq d \leq 3.15$  mm), different rotation speeds ( $20 \leq \omega \leq 40$  rpm) and a wall temperature of  $160^\circ\text{C}$ .

Activated alumina was selected as model material with regard to its pronounced hygroscopic behavior, its well known porosity and specific area and because the solid does not shrink or reacts chemically. Like for sewage sludge, the extended hot wire method [17] was used to determine the volumetric thermal capacity,  $\rho C_p$ , and the thermal conductivity,  $k$ . These physical properties as well as the apparent density are reported in **Erreur ! Source du renvoi introuvable.** for the various particle sizes. The sorption isotherm (Figure 5) and the total heat of sorption (Figure 6) were determined using the thermogravimetric analyzer (TGA) coupled with a differential scanning calorimeter DSC111 (Setaram, Caluire, France) for the 1 mm alumina beads.

The mixing number appears in the expression of the penetration resistance through the non dimensional apparent resting time. A sensitivity analysis of the contact and penetration resistances to the particle diameter, the moisture content and the stirring speed was performed to identify the optimal operating conditions, which allows to minimize the contact resistance and to maximize the penetration resistance. As can be seen in Figure 7, reduced sensitivity coefficients of the contact and penetration resistances to the particle diameter, are positive and negative, respectively. Consequently, optimal operating conditions are achieved for the smallest available particle size. The moisture content does not

exhibit any influence on the penetration resistance while the contact resistance linearly decreases when the moisture content decreases. Thus, the identification of the mixing number is better at low moisture content. In this range (low moisture content and small particle diameter), the stirrer speed has little influence on the contact resistance, as underlined in Figure 8, and any influence on the penetration resistance (Figure 9).

$\Psi$  and  $\xi$  were identified from drying experiments conducted with samples of about 650g of 1mm alumina balls, wetted to 0.32 kg/kg. The wall temperature was maintained at 160°C and the stirrer speed at 20 rpm. Steam was used as a sweeping gas. Adjustment constants suggested by Schlünder and Mollekopf [6] allow to adjust in a satisfactory way the experimental kinetic, as shown in Figure 10. Those values lead to a mixing number of 33.47.

## **IDENTIFICATION OF THE LIMITING MECHANISM**

Measured and computed drying kinetics for the digested sewage sludge coming from Albi City, processed with a dryer wall temperature maintained at 160°C and a stirrer speed at 40 rpm, are plotted in Figure 11. The decrease of the measured drying rate in the intermediate regime ( $0.32 \leq X \leq 3.2$  kg water/kg dry matter) results from the vertical design of the lab scale dryer, as previously explained. As the sludge is mainly dried by convection from superheated vapor and by conduction through the stirrer [1], the model could not describe this part of the curve. Nevertheless, it was not considered useful to modify the model since this intermediate regime is not observed in industrial paddle dryers. The evolutions of the measured and computed product temperature during drying are plotted in Figure 12. As long as the heated wall is fully covered by the product, the penetration model represents satisfactorily the experimental results. A characteristic dimension used to adjust the experimental results is equal to 1.15 mm. The relative deviation between the experimental results and the adjustment is lower than 13 % for the drying curve and lower than 7.5 % for the product temperature.

The model postulates that contact drying is a purely heat transfer controlled process, with “in series” resistances, i.e. the contact resistance and the penetration resistance of the bulk. The evolutions of the global, contact and bulk heat transfer coefficients are plotted in Figure 13. Down to moisture content of 1kg/kg dry matter, drying is exclusively controlled by the contact resistance. The influence of the penetration resistance of the bulk becomes significant only at lower moisture contents. Considering the determined characteristic dimension, this result is coherent with Schlünder and Mollekopf's observations [6] and with the sensitivity analysis previously described.

## **INFLUENCE OF THE OPERATING PARAMETERS ON THE KINETICS**

### **Influence of the dryer wall temperature**

The experimental and theoretical drying kinetics obtained for the digested sewage sludge from Albi City at two different dryer wall temperatures and a stirrer speed of 40 rpm are plotted in Figure 14. The characteristic dimension  $d=1.15$  mm, determined previously, is used for calculations. As can be seen in Figure 14, the model allows to find the influence of the dryer wall temperature in a relatively satisfactory way. To determine the influence of the temperature on the drying rate, we performed a numerical parametric study in the range  $120 \leq T \leq 180^\circ\text{C}$  for a stirrer speed of 40 rpm and a characteristic dimension of 1.15 mm. As expected, the drying rate was found to be linearly proportional to the dryer wall temperature and thus to the drying potential  $T_w - T_{\text{sat}}$ .

### **Influence of the stirrer speed**

Experimentally, as shown in Figure 15, Ferrasse and co-workers [2] identified a critical stirrer speed ( $\omega = 40$  rpm) beyond which an increase of the rotation speed did not affect the drying rate. The model proposed by Schlünder and Mollekopf [6] identifies an apparent resting time below which an increase of



the stirrer speed has no influence on the drying kinetic. The expression of this critical apparent resting time is given by the following relation:

$$t_{\text{critical}} = \frac{4}{\pi} R_{\text{contact}}^2 \left( \rho C_p k \right)_{\text{db}} \quad (16)$$

Knowing the mixing number, this equation allows to calculate the critical rotation speed. This leads to a critical value of 47 rpm, which is in accordance with experimental observations. It should be noticed that this value depends on the product through its thermophysical properties. To determine the influence of the stirrer speed on the drying rate, a numerical parametric study was performed in the range  $20 \leq \omega \leq 40$  rpm for a dryer wall temperature of 160°C and a characteristic dimension of 1.15 mm. We find that the drying rate increases with the stirrer speed according to the following relation:

$$F \propto \omega^{0.03} \quad (17)$$

Thus, the stirrer speed has little influence on F, at least for our dryer configuration.

#### Influence of the sludge characteristic dimension

The experimental and theoretical drying kinetics obtained for the digested sewage sludge and an extended aerated one at a dryer wall temperature of 160°C and a stirrer speed of 40 rpm are plotted in Figure 16. The characteristic dimensions used to adjust the experimental results are equal to 1.15 mm and 0.9 mm, respectively. By referring to the particle size distribution of the wet product plotted in Figure 1, it seems that this characteristic dimension corresponds to the size of the biggest particles contained in the dewatered sludge. To determine the influence of this characteristic dimension on the drying rate, a numerical parametric study was performed in the range  $0.5 \leq d \leq 2$  mm for a dryer wall temperature of 160°C and a stirrer speed of 40 rpm. The drying rate changes with the particle size according to the following relation:

$$F \propto d^{-0.53} \quad (18)$$

For the dryer design, a  $12\text{kg/m}^2\text{h}$  drying rate is typically assumed for a primary sludge while a value of  $18\text{kg/m}^2\text{h}$  is used for an extended aerated sludge. The ratio between these two empirical values (Table 3) is equal to the ratio of the theoretical drying rate, estimated with the size of the biggest particles in the wet sludge as the characteristic dimension. This result consolidates the hypothesis expressed previously.

## **SUMMARY**

The penetration theory developed by Schlünder and co-workers is used to improve our understanding of the mechanisms involved in contact drying of agitated sewage sludge. Simplifying hypotheses were formulated. The most binding assumption concerns the representation of pasty sludge by a mono-dispersed saturated particulate phase. As a consequence, the dry matter is assumed to be the same both in the pasty and granular regimes. The characteristic dimension of this pseudo-particulate phase is determined by adjustment of the experimental drying rate curves. A sensibility study of the model response - the drying rate - to the variations of the model parameters allowed to identify the most influent parameters, i.e. those that must be determined with the highest possible accuracy. Some of these parameters are linked to the product (the total heat of sorption, the thermal conductivity and the volumetric thermal capacity of the dry sludge) others to the dryer (the mixing number, the dryer wall temperature and the stirrer speed). A special attention was paid in the determination of the mixing number, which characterizes the dryer. Experiments were performed with mono-dispersed granular packing of activated alumina balls. Optimal operating conditions, which allows to minimize the contact resistance and to maximize the penetration resistance, were determined from sensitivity analysis of the contact and penetration resistances to the particle diameter, the moisture content and the stirring speed. Even though strong hypotheses were formulated, the extension of the penetration theory to pasty-like product allows to represent the experimental results in a satisfactory way and to understand the drying mechanisms involved in contact drying of agitated sewage sludge. The main conclusion is that drying is controlled by the contact resistance between the wall and the sludge, and especially between the wall and

the biggest particles contained in the dewatered sludge. The existence of a critical stirrer speed, which depends on the product to be dried, was documented. For the sewage sludge, this critical speed is close to 40 - 50 rpm. Anyway, the stirrer speed has little influence on the drying kinetic. As expected, the drying rate increase linearly with the drying potential  $T_w - T_{sat}$ . And finally, the drying rate is conversely proportional to the square root of the biggest particles diameter. This last result allows to find the empirical drying rates used for the dryer design.

## ACKNOWLEDGMENTS

The authors are grateful to the Midi-Pyrénées Region (France) for its financial supports during this work.

## NOMENCLATURE

a	Thermal diffusivity	$m^2 s^{-1}$
A	Adjustment constant used in (Eq. 16)	-
$C_{12}$	Overall radiation coefficient	-
$C_p$	Specific heat	$J kg^{-1} K^{-1}$
d	Particle size	m
D	Dryer diameter	m
F	Drying rate	$kg m^{-2} s^{-1}$
Fr	Froude number	-
g	Gravitational constant	$m s^{-2}$

$k$	Thermal conductivity	$\text{W m}^{-1} \text{K}^{-1}$
$l$	Modified mean free path of the gas molecules	$\text{m}$
$L_v$	Latent heat of vaporization	$\text{J kg}^{-1}$
$M$	Molecular weight	$\text{kg mol}^{-1}$
$N_{\text{mix}}$	Mixing number	-
$n$	Number of revolutions per second	$\text{s}^{-1}$
$P$	Pressure	$\text{Pa}$
$R$	Thermal resistance	$\text{m}^2 \text{K W}^{-1}$
$\tilde{R}$	Gas constant	$\text{J mol}^{-1} \text{K}^{-1}$
$t_r$	Apparent resting time	$\text{s}$
$T$	Temperature	$\text{K}$
$X$	Moisture content	$\text{kg kg}^{-1}$
$z$	Length normal to the heated wall	$\text{m}$

#### Greek letters

$\alpha$	Heat transfer coefficient	$\text{W m}^{-2} \text{K}^{-1}$
$\beta$	Parameter	
$\delta$	Surface roughness	$\text{m}$
$SF_j$	Sensibility coefficient	
$SF'_j$	Reduced sensitivity coefficient	$\text{kg m}^{-2} \text{s}^{-1}$
$\Delta H_{\text{total}}$	Total heat of desorption	$\text{J kg}^{-1}$
$\Delta T$	Increment of the temperature	$\text{K}$
$\Delta X$	Decrement of the moisture content	$\text{kg kg}^{-1}$
$\varepsilon$	Emissivity	-
$\Phi$	Surface coverage factor	-

$\gamma$	Accommodation coefficient	-
$\rho$	Density	$\text{kg m}^{-3}$
$\sigma$	Black body radiation coefficient	$\text{W m}^{-2} \text{K}^{-4}$
$\tau$	Reduced time	-
$\omega$	Stirrer rotation speed	rpm
$\psi$	Constant	-
$\zeta$	Constant	-

### Subscripts

adim	Reduced parameter
b	Bulk
db	Dry bed
m	Mean value
p	Particle
r	Resting
v	Vapor
water	Liquid water
w	Wall

### REFERENCES

- [1] Arlabosse, P.; Chavez, S.; Lecomte, D. Method for the thermal design of paddle dryers : Application to municipal sewage sludge, *Drying Technology* **2004**, 22 (10), 1-19.
- [2] Ferrasse, J.H.; Arlabosse, P.; Lecomte, D. Heat, Momentum and Mass Transfer Measurements in Indirect Agitated Sludge Dryer, *Drying Technology* **2002**, 20(4&5), 749-769.
- [3] Chavez, S. Séchage par contact avec agitation des boues résiduaires urbaines : influence de leur origine et des conditions opératoires sur la cinétique de séchage et les caractéristiques des boues sèches et des rejets gazeux, PhD Thesis, University of Perpignan, 2004, 187 p (in French).

- [4] Arlabosse, P. Penetration model for contact drying of agitated sewage sludge, *Chemical Engineering Transactions* **2005**, 7 (2), 701-706.
- [5] Wunschmann, J.; Schlünder, E.U. Heat transfer from heated surfaces to spherical packings, *International Chemical Engineering* **1980**, 20(4), 555-563.
- [6] Schlünder, E.U.; Mollekopf, N. Vacuum contact drying of free flowing mechanically agitated particulate material, *Chemical Engineering and Processing* **1984**, 18 (2), 93-111.
- [7] Tsotsas, E.; Schlünder, E.U. Contact drying of mechanically agitated particulate material in the presence of inert gas, *Chemical Engineering and Processing* **1986**, 20 (5), 277-285.
- [8] Tsotsas, E.; Schlünder, E.U. Vacuum contact drying of free flowing mechanically agitated multigranular packings, *Chemical Engineering and Processing* **1986**, 20 (6), 339-349.
- [9] Dittler, A.; Bamberger, T.; Gehrman, D.; Schlünder E.U. Measurement and simulation of the vacuum contact drying of pastes in a LIST-type kneader drier, *Chemical Engineering and Processing* **1997**, 36, 301-308.
- [10] Baudez, J.C; Ayol, A; Coussot, P. Practical determination of the rheological behavior of pasty biosolids, *Journal of Environmental Management* **2004**, 72, 181-188.
- [11] Ferrasse, J.H. Développement d'outils expérimentaux pour le dimensionnement de procédés de séchage conductif avec agitation : Application à des boues de stations d'épuration urbaines, PhD Thesis, University Paul Sabatier of Toulouse III, 2000, 195p (in French).
- [12] Vaxelaire, J.; Puiggali, J.R. Analysis of the drying of residual sludge: from the experiment to the simulation of a belt dryer, *Drying Technology* **2002**, 20(4&5), 989-1008.
- [13] Arlabosse, P.; Rodier, E.; Ferrasse, J.H.; Chavez, S.; Lecomte, D. Comparison between static and dynamic methods for sorption isotherm measurements, *Drying Technology* **2003**, 21 (3), 479-498.
- [14] Ferrasse, J.H.; Lecomte, D. Simultaneous heat-flow differential calorimetry and thermogravimetry for fast determination of sorption isotherms and heat of sorption in environmental or food engineering, *Chemical Engineering Science* **2004**, 59 (6), 1365-1376.
- [15] Bauer, R.; Schlünder, E.U. Effective radial thermal conductivity of packings in gas flow, *International Chemical Engineering* **1978**, 18, 181-204.
- [16] Kohout, M.; Collier, A.P.; Stepanek, F. Effective thermal conductivity of wet particle assemblies, *International Journal of Heat and Mass Transfer* **2004**, 47, 5565-5574.
- [17] Ladevie, B.; Fudym, O.; Batsale, J.C. A new simple device to estimate the thermophysical properties of insulating materials, *International Communication in Heat and Mass Transfer* **2000**, 27 (4), 473-484.
- [18] Gevaudan, A.; Andrieu, J. Contact drying modelling of agitated porous alumina beads, *Chemical Engineering and Processing* **1991**, 30 (1), 31-37.

**TABLE**

Table 1 - Thermal conductivity,  $k$ , and volumetric thermal capacity,  $\rho C_p$ , of the dry sewage sludge bed measured at 25°C

$k$ (W/m K)	$\rho C_p$ (J/m <sup>3</sup> K)	$C_p$ (J/kg K)
0.13	$1.3 \cdot 10^6$	$1130+2.8 T(^{\circ}\text{C})$

Table 2 - Thermal conductivity  $k$ , and volumetric thermal capacity  $\rho C_p$  and apparent density  $\rho$  of the dry alumina bed measured at 25°C

Particle diameter (m)	$k$ (W/m K)	$\rho C_p$ (J/m <sup>3</sup> K)	$\rho$ (kg/m <sup>3</sup> )
$3.15 \cdot 10^{-3}$	0.179	$1.5 \cdot 10^6$	911
$2.5 \cdot 10^{-3}$	0.158	$1.5 \cdot 10^6$	895
$2 \cdot 10^{-3}$	0.155	$0.9 \cdot 10^6$	888
$1 \cdot 10^{-3}$	0.154	$0.9 \cdot 10^6$	818

Table 3 - Ratio between the drying rates obtained for a digested sewage sludge and an extended aeration one.

	Extended aeration sludge	Primary sludge	Ratio
Empirical drying rate (kg/m <sup>2</sup> h) used for the dryer design	18	12	$\frac{18}{12} = 1.5$
Size of the biggest particles in the wet sludge (mm)	0.89	1.935	$\frac{(0.89)^{-0.53}}{(1.935)^{-0.53}} = 1.5$

**FIGURE**



Figure 1 – Particle size distribution of an extended aeration sludge (—□—), an anaerobically digested extended aeration sludge (—+—), an anaerobically digested sludge (—) and a primary one (—\*—) .

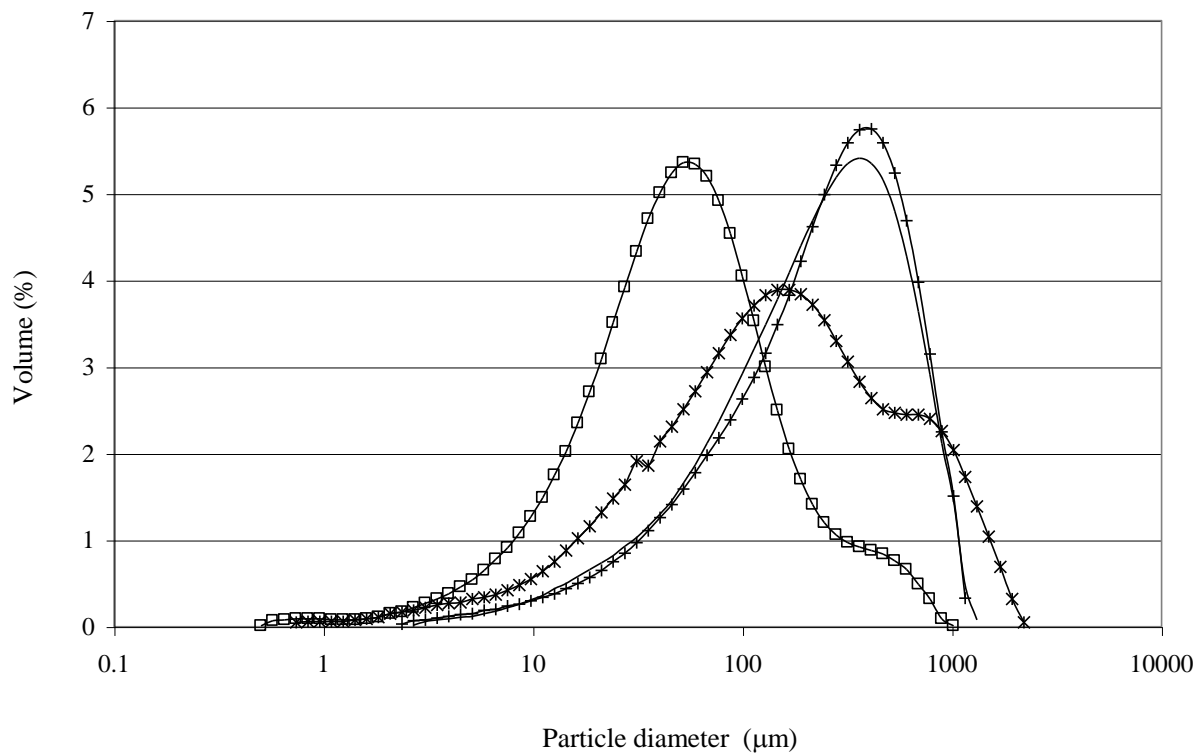


Figure 2 – Influence of the superheated vapor temperature, (+)  $T_{\text{vap}}= 120^{\circ}\text{C}$  and (o)  $T_{\text{vap}}= 135^{\circ}\text{C}$ , on the drying kinetic of the digested sewage sludge coming from Albi City ( $T_{\text{wall}} = 120^{\circ}\text{C}$ ,  $\omega = 60$  rpm).

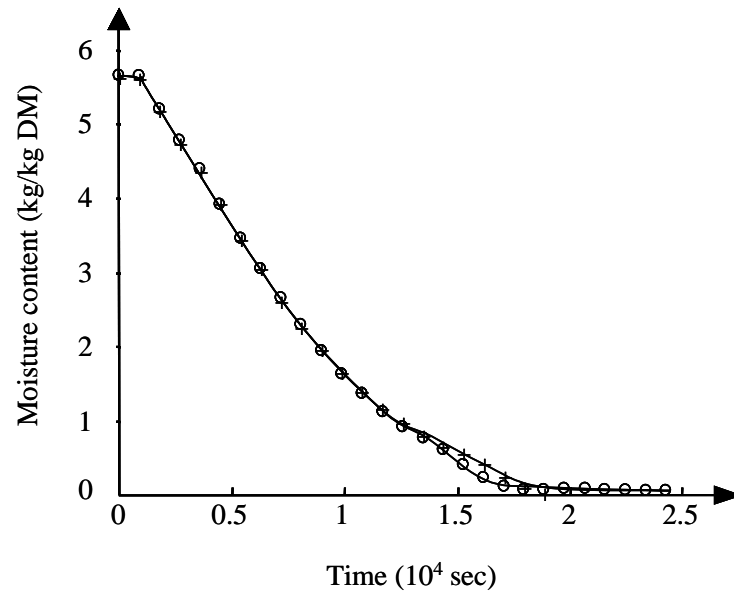


Figure 3 – Reduced sensitivity coefficients to parameters connected with operating conditions and wall properties : (—△—) wall temperature, (—◇—) stirrer speed, (—○—) mixing number, (—□—) surface coverage factor, (—) overall radiation coefficient.

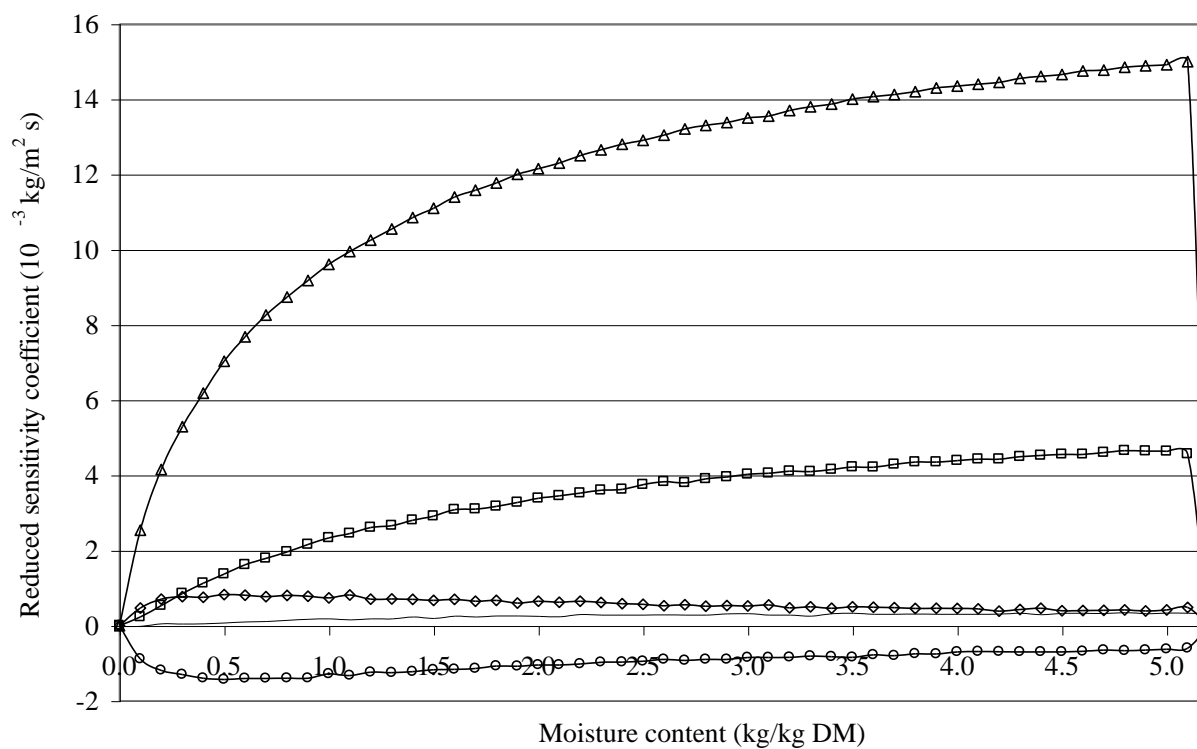


Figure 4 – Reduced sensitivity coefficients to parameters connected with product properties : (—+—) particle diameter, (—○—) particle rugosity, (—□—) thermal conductivity,(—△—) specific heat and (—) apparent density.

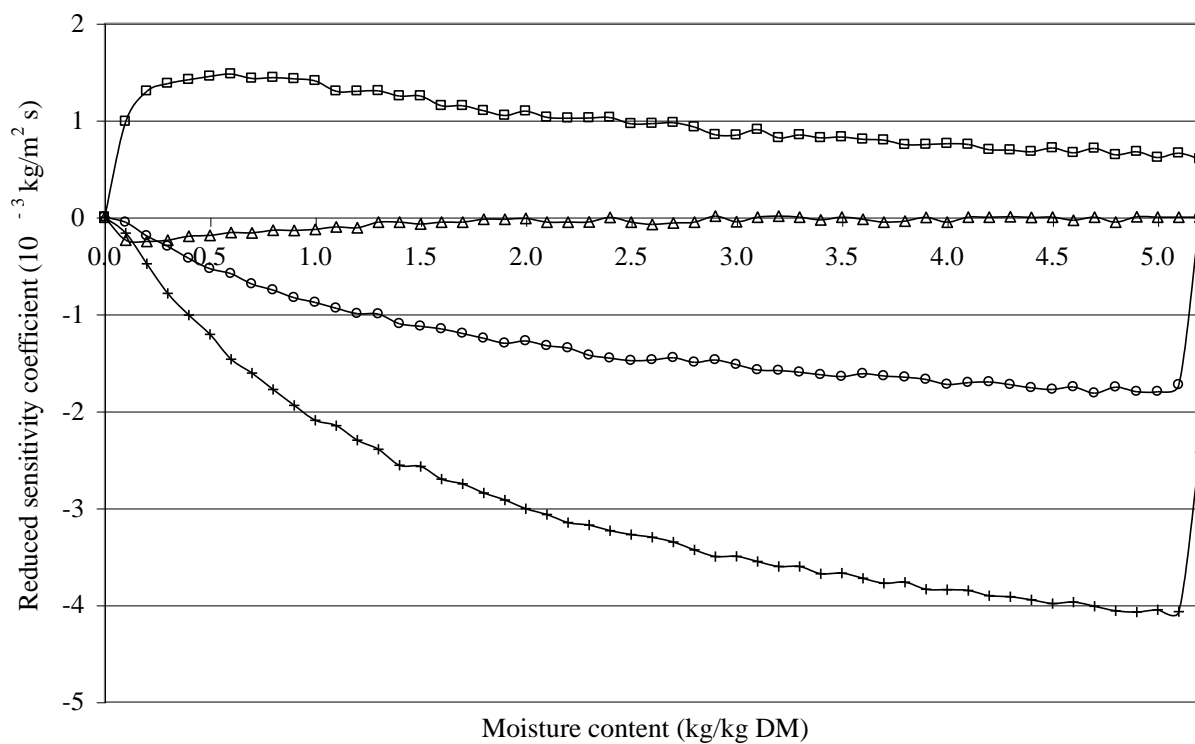


Figure 5 – Activated alumina desorption isotherm measured at 95°C (three replicates).

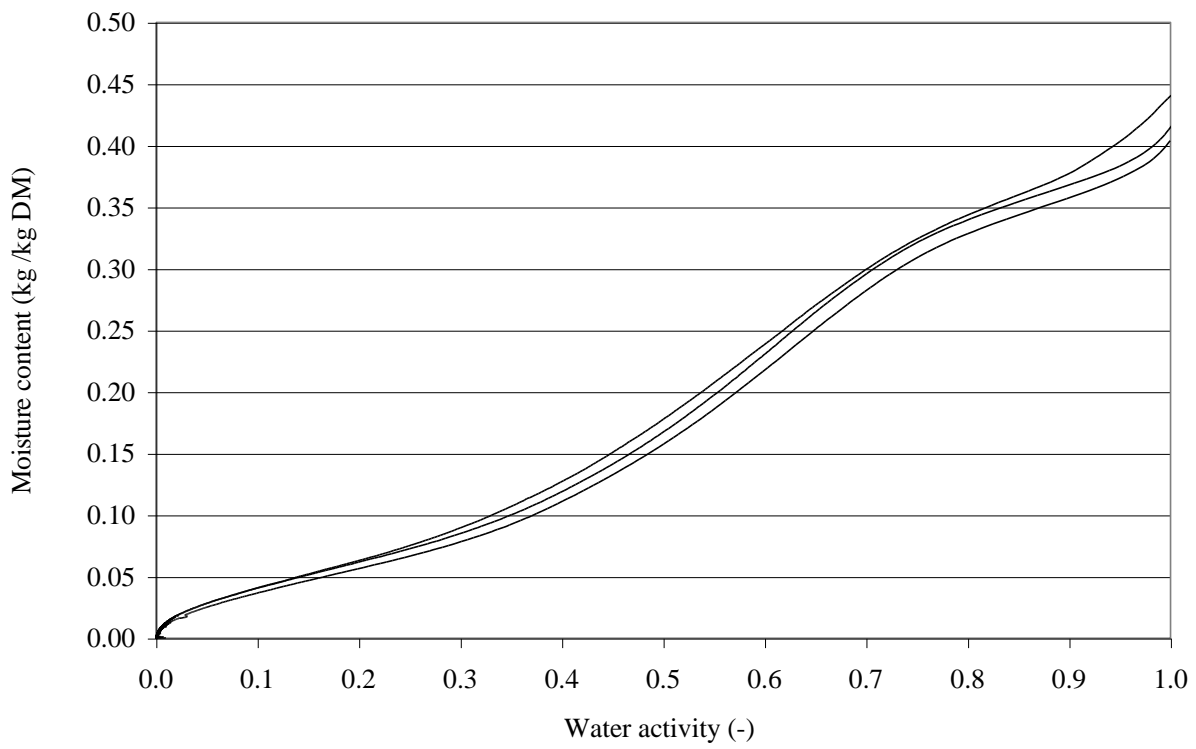


Figure 6 – Activated alumina total heat of desorption measured at 95°C (three replicates).

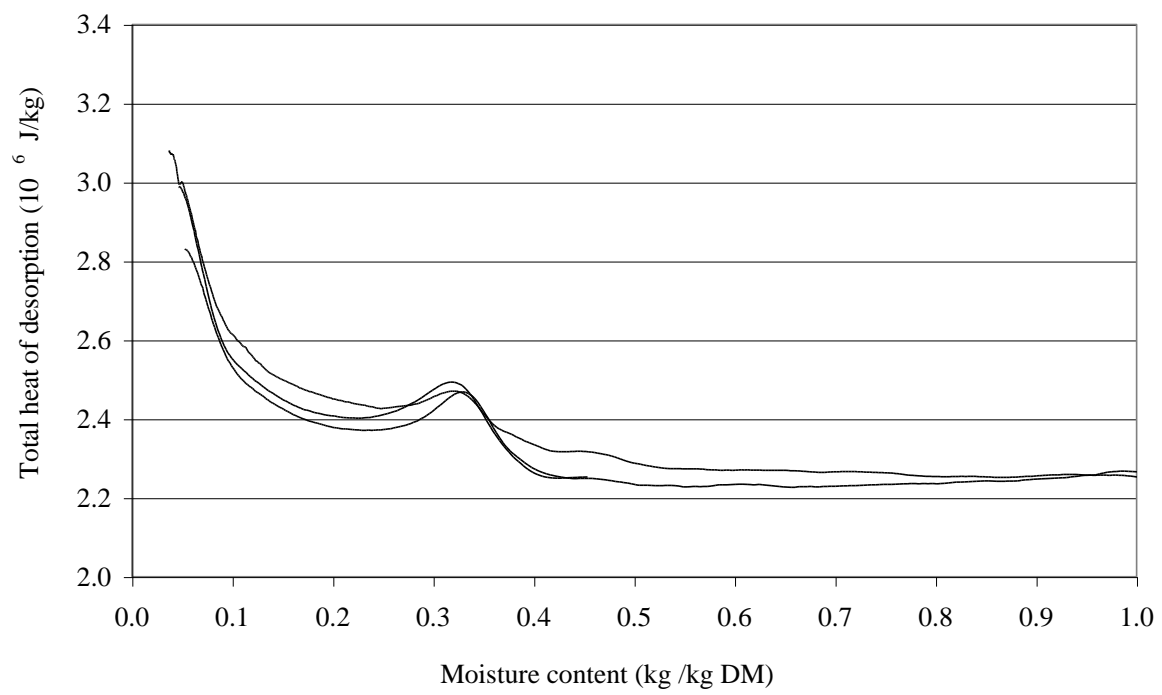


Figure 7 – Reduced sensitivity coefficients of the penetration resistance ( $\text{---}\ominus\text{---}$ ) and the contact one ( $\text{---}\square\text{---}$ ) to the particle diameter.

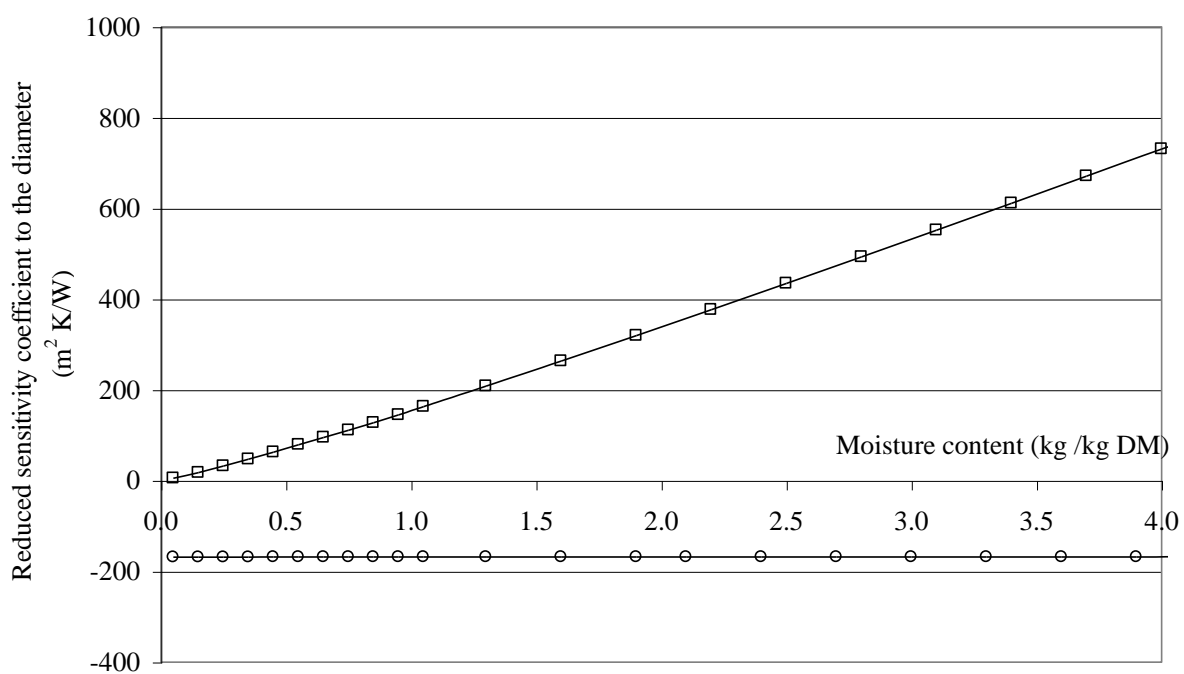


Figure 8 – Reduced sensitivity coefficients of the contact resistance to the stirrer speed and the moisture content for  $10^{-3}$  m activated alumina balls.

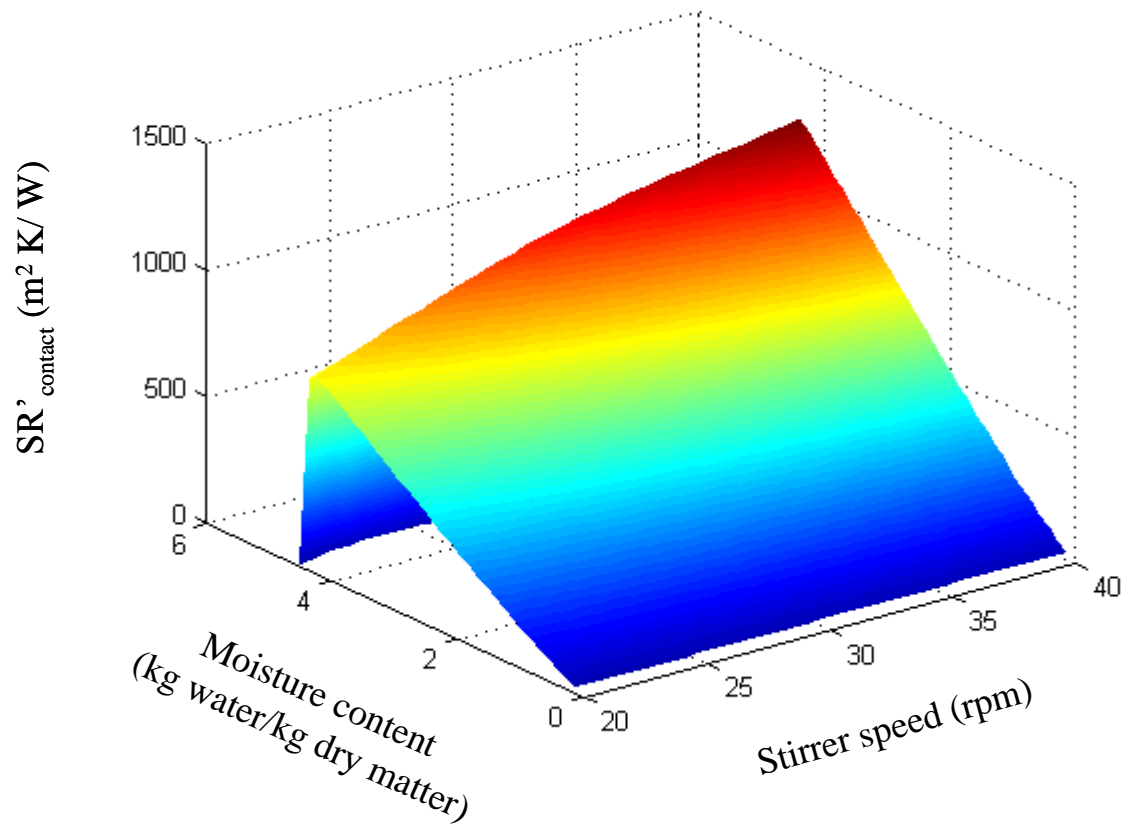




Figure 9 – Reduced sensitivity coefficients of the penetration resistance to the stirrer speed and the moisture content for  $10^{-3}$  m activated alumina balls.

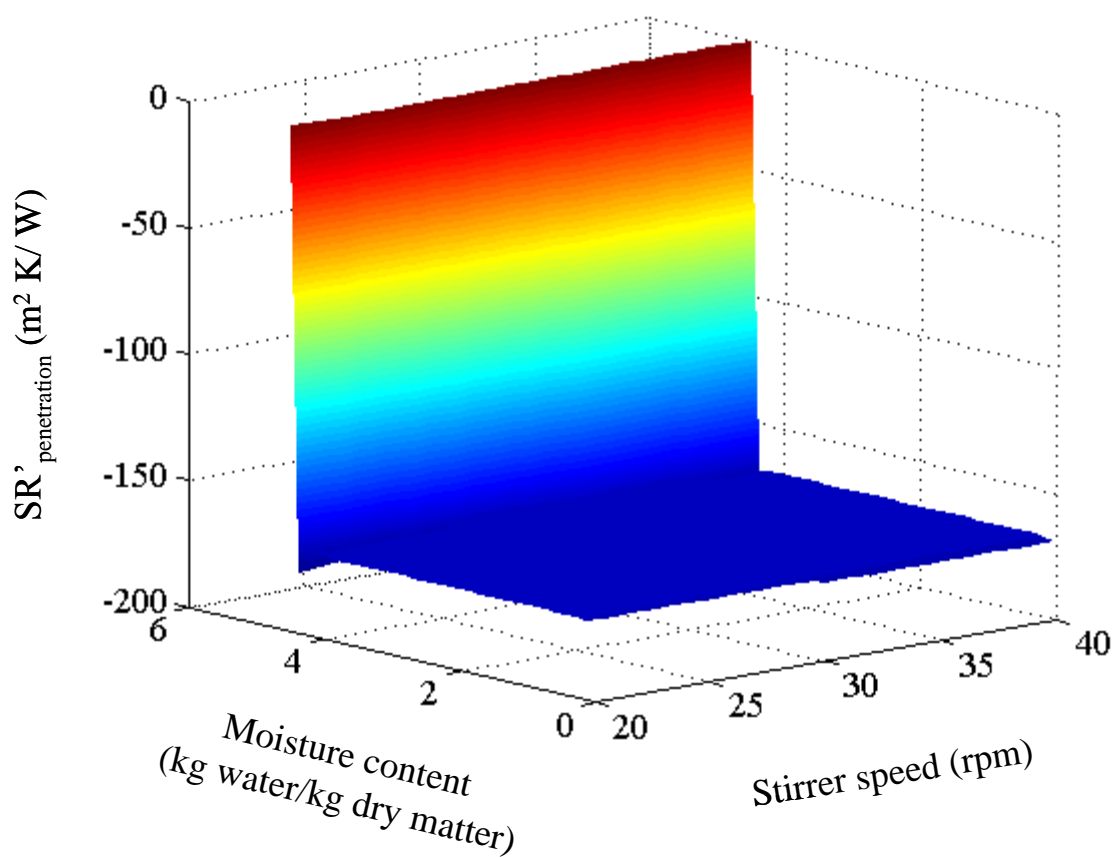


Figure 10 – Experimental (dot) and adjusted (line) drying kinetics of activated alumina balls ( $d=10^{-3}\text{m}$ ,  $T_{\text{wall}} = 160\text{ }^{\circ}\text{C}$ ,  $\omega = 20\text{ rpm}$ ).

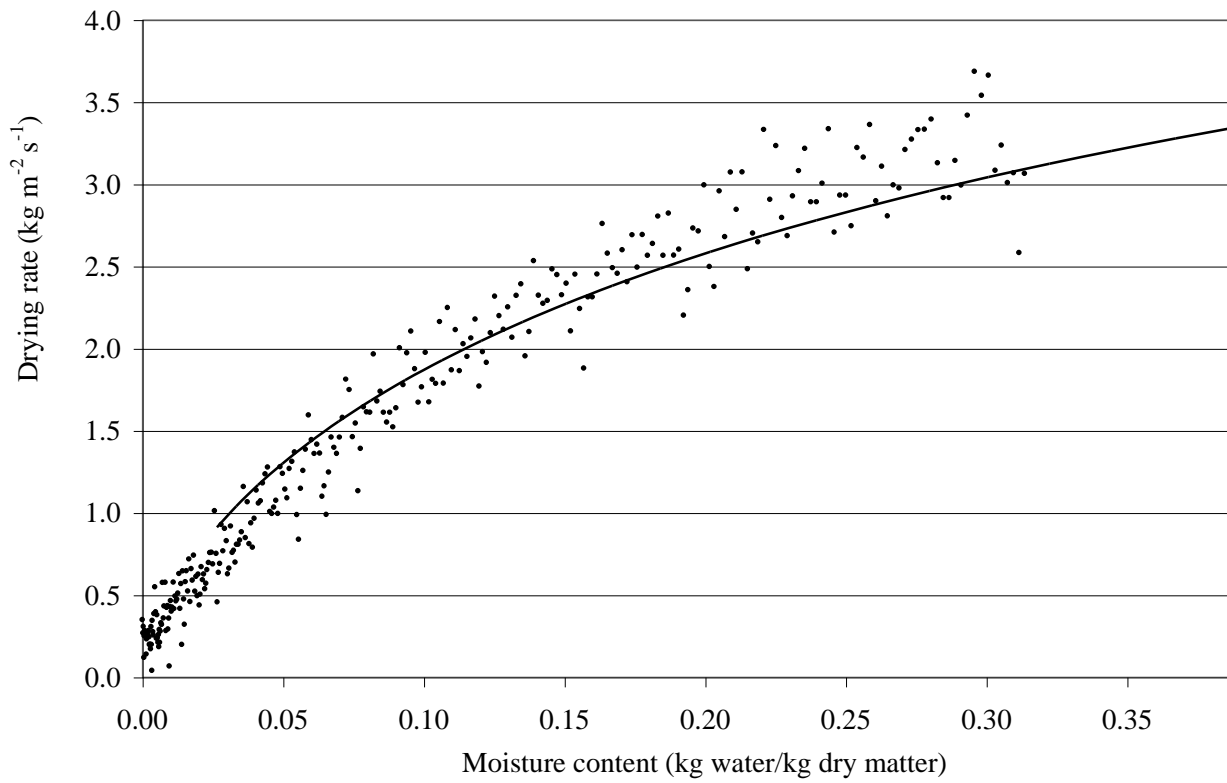


Figure 11 – Measured (—) and adjusted (—□—) drying kinetics of the digested sewage sludge coming from Albi City ( $T_{\text{wall}} = 180^{\circ}\text{C}$ ,  $\omega = 40 \text{ rpm}$ ,  $d = 1.15 \cdot 10^{-3} \text{ m}$ ).

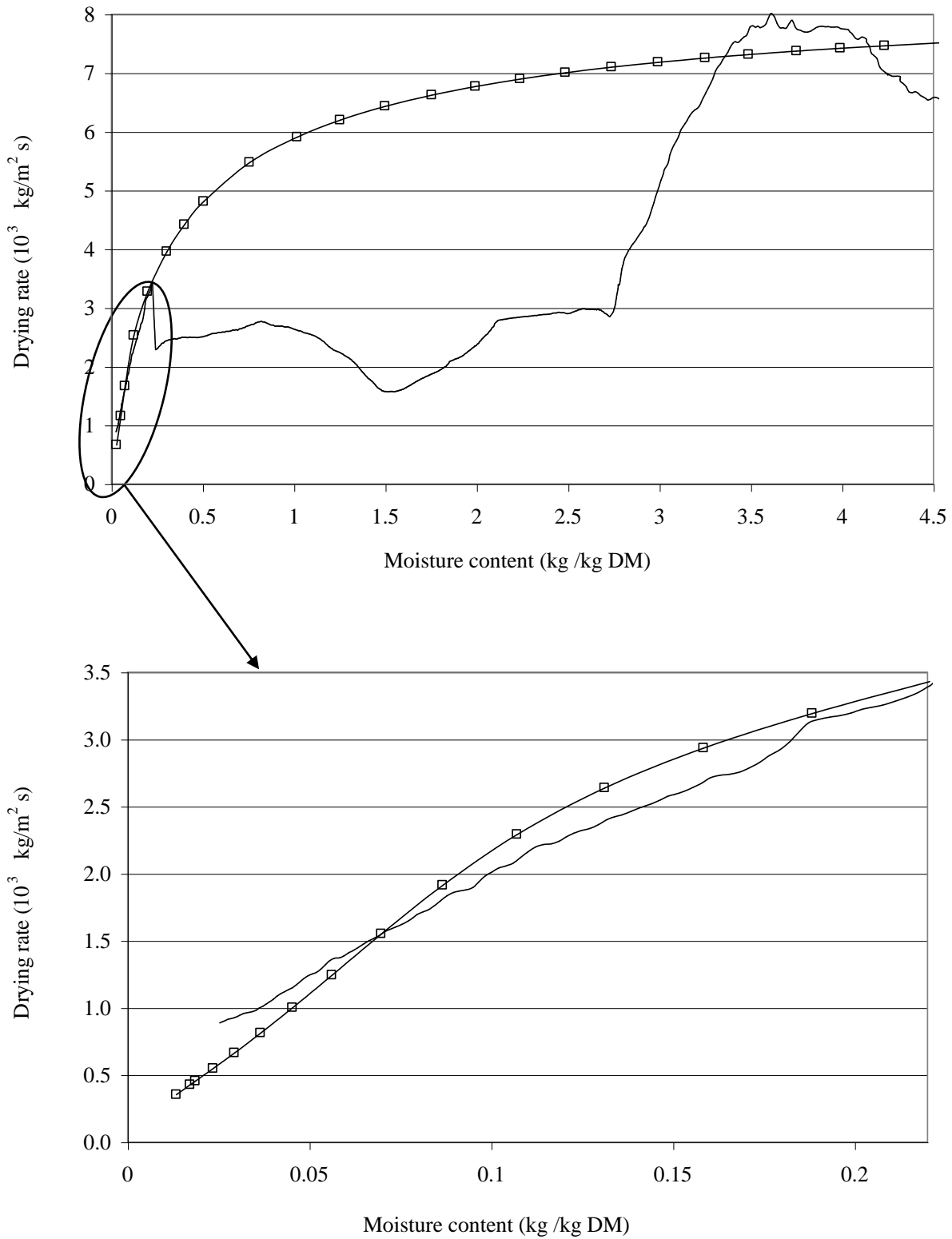


Figure 12 – Measured (—) and computed (—□—) product temperature ( $T_{\text{wall}} = 180^{\circ}\text{C}$ ,  $\omega = 40$  rpm,  $d = 1.15 \cdot 10^{-3}$  m).

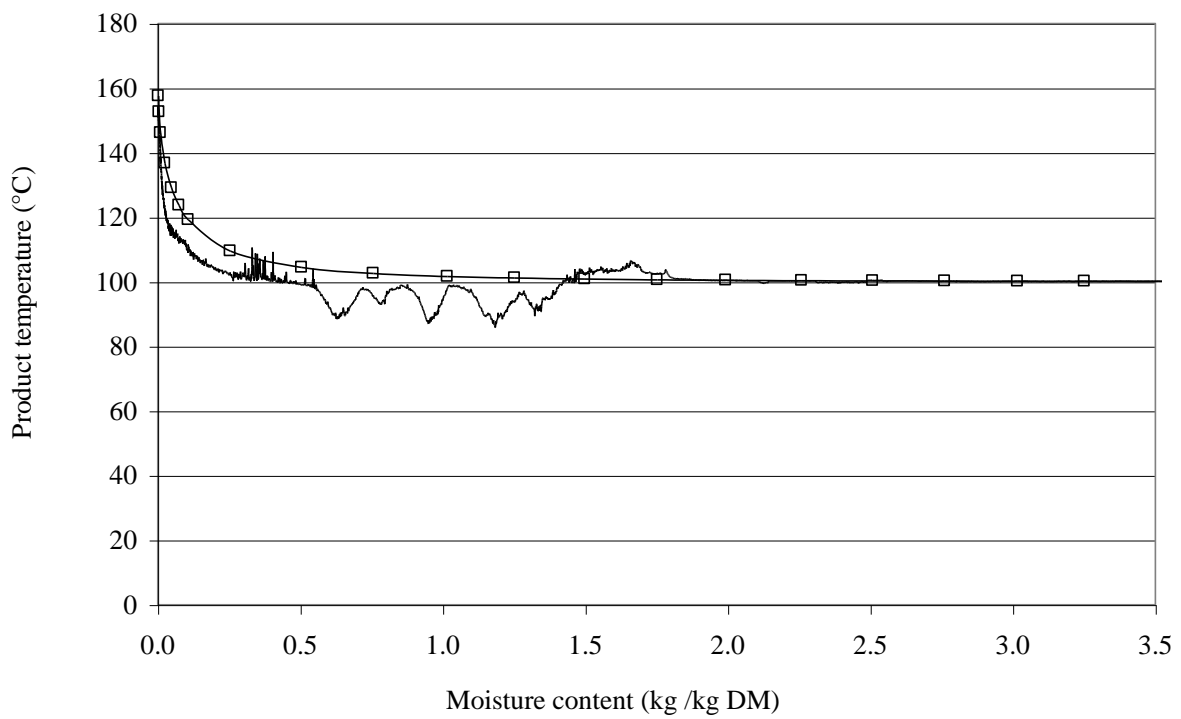


Figure 13 – Evolution of the global (□), contact (○) and bulk (✱) penetration resistances with the moisture content ( $T_{\text{wall}} = 180^{\circ}\text{C}$ ,  $\omega = 40$  rpm,  $d = 1.15 \cdot 10^{-3}$  m).

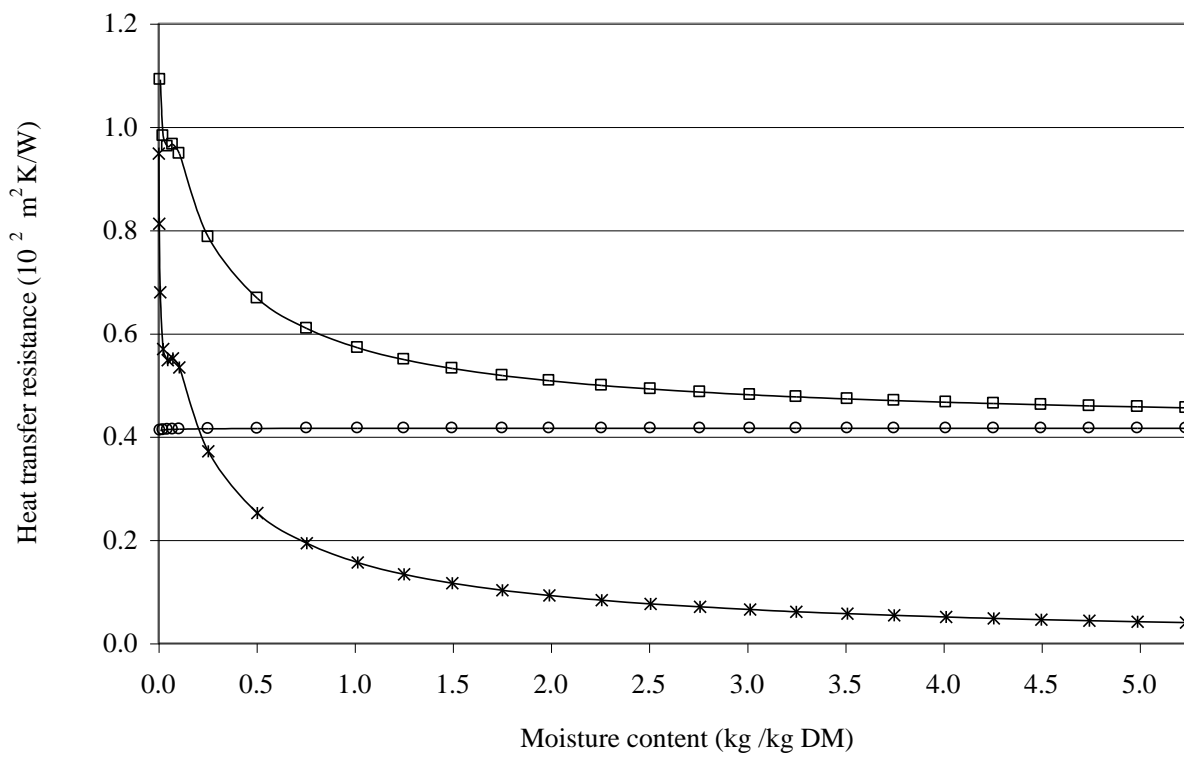


Figure 14 – Measured (dot) and adjusted (line) drying kinetics of the digested sewage sludge coming from Albi City for (□)  $T_{\text{wall}} = 160^{\circ}\text{C}$  and (○)  $T_{\text{wall}} = 120^{\circ}\text{C}$  ( $\omega = 40$  rpm,  $d = 1.15 \cdot 10^{-3}$  m).

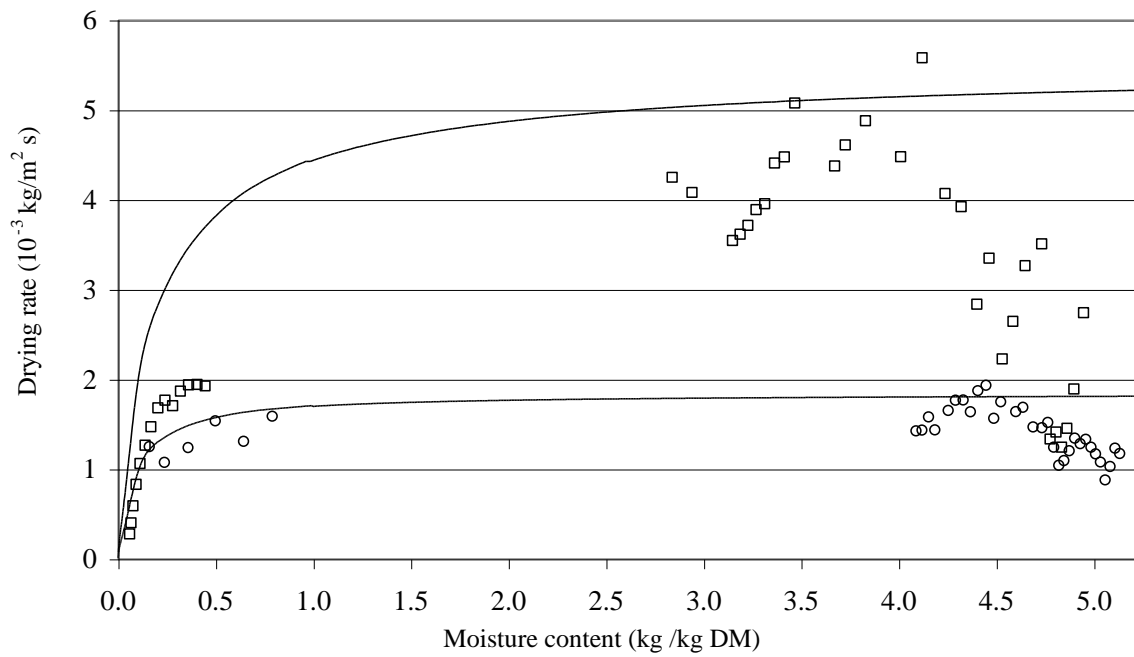


Figure 15 – Influence of the stirrer speed, (+)  $\omega = 20$  rpm, (o)  $\omega = 40$  rpm and (--)  $\omega = 60$  rpm, on the experimental drying kinetic ( $T_{\text{wall}} = 120^\circ\text{C}$ ).

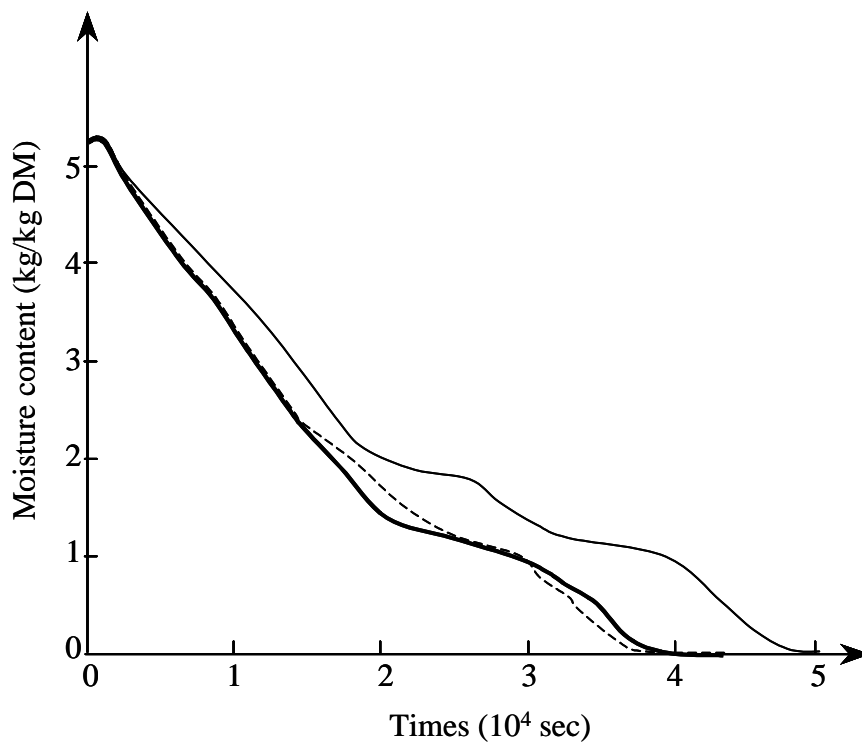


Figure 16 Measured (dot) and adjusted (line) drying kinetics of an anaerobically digested sludge ( (+),  $d=1.15 \cdot 10^{-3}$  m) and an extended aeration one (  $\circ$ ),  $d=0.9 \cdot 10^{-3}$  m) for  $T_{\text{wall}} = 160^\circ\text{C}$  and  $\omega = 40$  rpm.

